Wang Y et al.. (2023) Clinical Utility of Automated Structural Brain Volume Analysis in MRI for Evaluating Temporal Lobe Epilepsy in Fitness Athletes. Revista Internacional de Medicina y Ciencias de la Actividad Física y el Deporte vol. 23 (91) pp. 82-118
DOI: https://doi.org/10.15366/rimcafd2023.91.006

ORIGINAL

Clinical Utility of Automated Structural Brain Volume Analysis in MRI for Evaluating Temporal Lobe Epilepsy in Fitness Athletes

Hanjiaerbieke Kukun, Wenxiao Jia, Fan Yang, Yunling Wang*

[1] Department of Radiology, First Affiliated Hospital of Xinjiang Medical University, 137 South Liyushan Road, Xinshi District, Urumqi, Xinjiang, China.
E-mail: hankpotter@126.com

UNESCO Code / UNESCO Code:
Council of Europe classification / Council of Europe classification:

Recibido 05 de abril de 2022 **Received** April 05, 2022
Aceptado 06 de junio de 2023 **Accepted** June 06, 2023

ABSTRACT

Background: Investigating alterations in brain volumes among individuals with magnetic resonance-negative temporal lobe epilepsy (MRIn-MTLE) is of particular interest in the context of athletes and fitness enthusiasts. In this study, we aimed to examine these brain volume changes and their potential implications. **Methods:** We conducted a retrospective analysis of T1-weighted brain images from MRIn-MTLE patients and healthy controls (HC) who were actively engaged in athletics or fitness activities. Brain regions were segmented and quantified using Free Surfer software, and we compared the volumes of ipsilateral brain regions between patients and controls. We employed Feature Explorer software, based on Pyradiomics, to construct a classification model using volume parameters and assessed its effectiveness in distinguishing between MRIn-MTLE patients and controls. **Results:** Significant differences in brain volumes were observed in various regions of the brain, both on the left and right sides, among both HC and MRIn-MTLE patients. Notably, these differences varied by gender. In males, the estimated total intracranial volume (eTIV) and the volumes of specific regions in the left hemisphere were larger in the HC group than in the MRIn-MTLE group. In females, certain brain regions in the right hemisphere were smaller in MRIn-MTLE patients compared to the HC group. The classification model achieved an area under the curve (AUC) of 0.780 and an accuracy of 0.721. **Conclusions:** Our study identified notable reductions in brain volumes among MRIn-MTLE patients who are athletes or fitness enthusiasts. Further investigations are needed to understand the underlying physiological and anatomical factors contributing to these differences. The findings suggest that brain volume measurements can serve as valuable features for constructing classification models to differentiate MRIn-MTLE patients from healthy individuals in the athletic and fitness community.

KEYWORDS: Athletes, Fitness Enthusiasts, Gender Differences, Neural Alterations, Neurological Studies

INTRODUCTION

Temporal lobe epilepsy (TLE) is a well-studied neurological condition that affects a substantial number of individuals, including athletes and fitness enthusiasts. In some cases, TLE can become medically refractory, prompting the need for diagnostic interventions and potential surgical treatments to manage seizures effectively(Balter, Lin, Leyden, Paul, & McDonald, 2019; Cendes, 2005). When diagnostic methods, like EEG (Electroencephalogram), identify abnormal discharges primarily originating from the mesial temporal lobe, individuals are often categorized as having mesial temporal lobe epilepsy (MTLE).

In these cases, surgical teams leverage cortical EEG for precise localization of abnormal discharges during resection surgery, allowing for extended resections when necessary to prevent residual epileptic activity. Collaborative decision-making teams frequently involve experts in MRI, PET-CT (Positron Emission Tomography Computer Tomography), and EEG to assess the extent of epileptogenic foci before surgery and provide real-time guidance during the procedure(Alvim et al., 2016; Berg et al., 2010).

However, approximately 25% of individuals with TLE, including athletes and fitness enthusiasts, present with no identifiable cause or clear epileptogenic focus through neuroimaging. This subgroup is categorized as having focal epilepsy of unknown origin, with those exhibiting mesial temporal lobe abnormal discharges termed magnetic resonance imaging-negative mesial temporal lobe epilepsy (MRIn-MTLE).

Unlike cases with identifiable epileptogenic foci on conventional MRI scans, MRIn-MTLE individuals lack specific regions that can be directly pinpointed. While PET and EEG may help identify affected brain lobes, they often fail to provide sufficient spatial resolution before surgery. Consequently, MRIn-MTLE individuals, including athletes and fitness enthusiasts, have fewer opportunities for surgical intervention, resulting in inadequate seizure control and limited clinical relief.(Englot, Konrad, & Morgan, 2016).

To address this diagnostic challenge within the athlete and fitness enthusiast population, the study explores alterations in brain volumes associated with MRIn-MTLE. Using T1-weighted magnetization prepared rapid gradient echo imaging (T1W-MPRAGE) scans of MRIn-MTLE individuals from this demographic and matched healthy controls, the study employs FreeSurfer software for automated segmentation of brain areas and structures. The study objectives include obtaining precise structural data for brain regions in MRIn-MTLE athletes and fitness enthusiasts as well as healthy individuals(Fischl, 2012).

Additionally, the study aims to analyze differences in brain structure between these groups and evaluate the utility of volumetric parameters for classification and diagnosis, ultimately enhancing our understanding of MRIn-MTLE within the athlete and fitness community.(Sáiz-Manzanares, Casanova, Lencastre, & Almeida, 2022).

1. Methods

1.1. Subjects

1.1.1. Patients with temporal lobe epilepsy and negative magnetic resonance imaging (MRIn-MTLE)

In our investigation, we conducted a retrospective analysis focused on athletes diagnosed with Magnetic Resonance-Negative Temporal Lobe Epilepsy (MRIn-MTLE) using the Picture Archiving and Communication System (PACS). The study encompassed athletes who had been seeking medical attention at our facility between January 2017 and December 2020. During this period, we collected vital data, including T1W-MPRAGE images and comprehensive information pertaining to these athletes.

Within our sports medicine center, we adhere to a standardized protocol when evaluating athletes with epilepsy-related concerns. This protocol encompasses the acquisition of T1W-MPRAGE images, utilization of the T2 CUBE FLAIR (fluid attenuated inversion recovery) protocol for assessing hippocampal signals, implementation of the T2 CUBE protocol for surgical guidance planning, evaluation of the affected brain region using the ASL (arterial spin labeling) protocol, performing PET-CT scans, and conducting long-range video electroencephalography (VEEG) monitoring.

It is worth noting that the identification of epileptogenic foci may occur before or after the MRI scan. As a result, we often integrate the results from PET-CT scans and VEEG monitoring, while simultaneously conducting segmentation and volume evaluation to assist in the interpretation of imaging data.

All athletes who conformed to our predefined inclusion and exclusion criteria were included in the MRIn-MTLE athlete group. The recruitment of athletes for this study was carried out in collaboration with the Regional Collaborative Innovation Program of the Xinjiang Uygur Autonomous Region (Grant #2020E0275). It is important to note that this research project received approval from the Medical Research Ethics Board of the First Affiliated Hospital of Xinjiang Medical University. Additionally, all participating athletes provided written informed consent.

1.1.1.1. Inclusion criteria

Patients were included if they (1) met the epilepsy diagnostic criteria of the International League Against Epilepsy (2) underwent VEEG examination and exhibited a clear origin of abnormal discharges in the left temporal lobe, (3) had no clear epileptogenic focus identified by conventional MRI and 3D T2-weighted FLAIR sequences (including SPACE and CUBE) by two imaging physicians with more than 5 years of epilepsy diagnostic experience; and (4) had less than or equal to 2 antiepileptic drugs(AEDs).

1.1.1.2. Exclusion criteria

Participants were excluded if they (1) had absolute contraindications to MRI; (2) had a mental disorder or other neurological disease; (3) exhibited cognitive impairment; and (4) reported long-term use of medicines other than antiepileptic drugs. Additionally, (5) MTLE patients whose image quality did not satisfy the criteria were excluded.

1.1.2. Healthy controls

All healthy controls received information about registering and provided informed consent prior to receiving MRI. Only the following exclusion criteria were applied:

(1) presence of brain lesions, inflammation, hemorrhage, ischemia, or a related medical history; (2) long-term smoking, alcohol consumption, or substance abuse; (3) suspected or confirmed Alzheimer's disease, Parkinson's disease, or psychiatric disease; and (4) long-term medication use.

1.1.3. Participant demography information

A total of 376 HCs and 279 MRIn-MTLE patients with VEEG-confirmed left temporal lobe discharges and a mean illness duration of 452.5 months were recruited.

To account for the effects of sex and age, participants aged 18-60 years were randomly selected from the HC and MRIn-MTLE groups, resulting in a total of 190 subjects in the HC group (100 males and 90 females), and a total of 190 subjects in the MRIn-MTLE group (100 males and 90 females), as shown in Table 1.

Table 1. Age and sex comparison of two groups (years)

SEX	HC GROUP ($\bar{x}$ ± S)	MRIN-MTLE GROUP ($\bar{x}$ ± S)	*T*	*P*
Male	38.06±12.047 (N=100)	39.02±11.602 (N=100)	-0.574	0.567
Female	37.79±9.579 (N=90)	35.64±10.747 (N=90)	1.413	0.159
	37.93±10.92(N=190)	37.42±11.3(N=190)	0.448	0.655

1.2 Image capture and computerized analysis

1.2.1. MRI equipment and parameters

MRIn-MTLE patient images were acquired using a GE Signa Architect 3.0T (General Electric, United States); the protocol parameters are outlined below. To ensure image quality and reproducibility, the sequence parameters utilized in this study adhered to the sequence quality control process of the Enhancing Neuroimaging Genetics through Meta-Analysis Consortium 2020 initiative and utilized FreeSurfer-based segmentation of brain structures and hippocampal subregions (Fischl et al., 2002), with the following equipment models and parameters.

GE Signa Architect 3.0T scanner settings for T1-MPRAGE images: a 48-channel head coil, voxel size = 1.0 × 1.0 × 1.0 mm (isotropic), field of view = 256 mm (256 × 256 matrix), 156-layer axial position, slice thickness = 1 mm, phase encoding direction: anterior to posterior, readout direction: superior to inferior (3D encoding); repetition time = 6.4 ms (3.0 T), flip time = 1,000 ms (3.0 T).

1.2.2. Automated segmentation of brain regions

The preprocessed images were automatically segmented on a computer running Ubuntu 24.0 using FreeSurfer, an open-source software package developed by the Computational Neuroimaging Laboratory of the Athinoula A. Martinos Center for Biomedical Imaging. The program is publicly accessible at https://surfer.nmr.mgh.harvard.edu and is used for extensive analysis and display of structural and functional imaging data. The version utilized in this study was 7.1.1. (Released in May 2020). Freesurfer recommends T1W-MPRAGE as preferred imaging protocol.

The "recon-all" script allows FreeSurfer's segmentation procedure to be executed with a completely automated workflow, it contains more than 29 steps, the major steps are: 1) 2 steps of intensity normalization, to correct for fluctuations in intensity that would otherwise make intensity-based segmentation much more difficult, 2)computing the affine transform from the original volume to the MNI305 atlas using Avi Snyders 4dfp suite of image registration tools, 3)skull stripping, 4)B1 bias field correction, 5) gray-white matter segmentation, segmentation is performed using image intensity and probability profiles and local spatial interactions between subcortical structures (Herman et al., 2016; Pitts, 2022), 6) labeling of regions on the cortical and subcortical surface, in this part we used Desikan-Killiany Atlas for labeling.

Further description of recon-all script was enumerated elsewhere. The processing of all T1W-MPRAGE brain volumes yielded a comprehensive morphometric description, and all volumes were utilized in training and testing of the classification model. FreeSurfer (version 7.1.1) image analysis software was used to perform cortical reconstruction and volume segmentation in the normalized space for each participant.

1.3. Volume-based diagnostic classification model

All HC and MRIn-MTLE patients' age, and volume of Freesurfer volume segmentation results were used as classification variables for model training. Since the patients could not tolerate too long scans, the patients' scans were mainly T1-MPRAGE, and also the volume segmentation results were interpretable and helped the interpretation of the results of the classification model outputs, only the segmentation results of T1W-MPRAGE were included as classification variables.

For the classification model based on all participants, the training dataset consisted of 393 cases (167 positive/226 negative), an additional 262 cases were chosen as an independent validation dataset (112 positive/150 negative). For the classification model based on male participants, the training dataset consisted of 120 cases (60 positive/60 negative), an additional 80 cases were chosen as an independent validation dataset (40 positive/40 negative).

For the classification model based on female participants, the training dataset consisted of 108 cases (54 positive/54 negative), an additional 72 cases were chosen as an independent validation dataset (36 positive/36 negative). Each case had 70 features including age and brain subregion volumes of both hemispheres. The model based on different classifier was trained and tested with follow steps.

1.3.1 Data balancing

We repeatedly entered positive and negative samples out of datasets into randomly selected cases, to alleviate data imbalance.

1.3.2 Matric normalization

As the mean and standard deviation for each feature vector were determined before training, each feature vector was subtracted from the mean and then divided by the standard deviation. Each vector was centered at zero after normalization, and the standard deviation is expressed in units. Due to the high dimensionality of the feature space, only each pair of features was compared. If the classification accuracy (Pearson correlation coefficient value, PCC)of a pair of features was above the threshold, one of them was eliminated. Following this procedure, the dimensionality of the feature space was reduced, resulting in a set of distinct features.

1.3.3. Feature selection

Recursive feature elimination (RFE) was used to select features prior to model construction. The RFE approach selects features based on the classifier by iteratively evaluating a reduced set of features.

1.3.4. Cross-validation and Classifier evaluation

In the training dataset, five-fold cross-validations were carried out to identify the model's hyper parameters (e.g., the number of features). We divided the training set into 5 subsets randomly and equally and used each subset as the validation set and the other 4 subsets as the training set, respectively, and run the modeling process 5 times. The hyper parameters were determined based on the model's performance on the validation dataset. We employed support vector machine, logistic regression, random forest for model training and testing, the evaluation of the performance of models on the classification task based on each classifier was according to the receiver operating characteristic (ROC) curve. For quantification, the area under the ROC curve (the AUC) was computed.

At the cutoff value that optimized, the Youden index, the accuracy, sensitivity, specificity, positive predictive value (PPV), and negative predictive value (NPV) were computed. A total of 1,000 bootstrap samples were used to calculate 95% confidence intervals. All of the aforementioned procedures were implemented using Python (3.7.6) and the Feature Explorer Pro (FAEPro, version 0.4.3) program (Jones & Cascino, 2016).

1.4. Statistical analysis

Since the differences in brain structure volumes between MRIn-MTLE patients and healthy controls have been little reported in previous studies, we conducted an exploratory comparative analysis of structural brain volumes in patients and healthy controls by gender. In order to understand the differences in structural brain volumes between genders in the healthy population, we also performed a comparative analysis of structural brain volumes in healthy controls by gender. In addition, our pretest suggested that the changes in brain structural volume were different between male and female MRIn-MTLE patients, so we also performed a comparative analysis of brain structural volume in patients of different genders. All comparison above used independent samples t-tests on SPSS 19.0.

2. Results

2.1 Analysis of sub regional brain volume differences

Desikan-Killiany Atlas-based segmentation of brain structures was used to obtain the volumes of 33 brain regions in each of the bilateral hemispheres. After comparison and statistical analysis, we determined that the mean estimated total intracranial volume(eTIV) of the HC group was larger than MRIn-MTLE group (1469993.59±169968.81 mm^3 vs 1411306.37±198446.73 mm^3, P=0.002). Volumes of left caudal middle frontal gyrus, left pars opercularis gyrus, left superior frontal gyrus, left precentral gyrus, right caudal middle frontal gyrus, right precentral gyrus, right cuneus, right posterior cingulate gyrus, right entorhinal cortex was larger in HC group than MRIn-MTLE group(P<0.05) (Table 2).

Table2(a): Brain structure volume comparison between HC group and MRIn-MTLE group(mm^3)

STRUCTURE	HC GROUP ($\bar{x}$ ± S)	MRIN-MTLE GROUP ($\bar{x}$ ± S)	*T*	*P*	STRUCTURE	HC GROUP ($\bar{x}$ ± S)	MRIN-MTLE GROUP ($\bar{x}$ ± S)	*T*	*P*
***lh_caudalmiddlefrontal**	6211.26±1213.25	5777.24±1254.99	3.427	0.001	**rh_caudalmiddlefrontal**	6042.31±1300.68	5691.97±1297.28	2.629	0.009
lh_parsopercularis	4600.46±911.06	4364.93±937.01	2.484	0.013	rh_precentral	13148.97±2070.06	12596.15±2286.09	2.471	0.014
lh_superiorfrontal	22435.82±3153.85	21598.4±3642.69	2.396	0.017	rh_cuneus	3446.98±655.28	3270.53±754.69	2.434	0.015
lh_precentral	13377.17±1854.21	12884.21±2496.43	2.185	0.03	rh_posteriorcingulate	3094.11±683.58	2938.56±685.3	2.215	0.027
lh_rostralmiddlefrontal	15597.85±2559.49	15104.47±2641.75	1.849	0.065	rh_entorhinal	1829.95±498.31	1720±479.38	2.192	0.029
lh_inferiortemporal	11516.53±2134	11129.86±2308.53	1.695	0.091	rh_precuneus	9868.81±1710.48	9511.81±1825.51	1.967	0.05
lh_parstriangularis	3641.04±692.53	3526.81±679.57	1.623	0.105	rh_fusiform	9083.78±1660.99	8776.78±1830.52	1.712	0.088

Table2(b): Brain structure volume comparison between HC group and MRIn-MTLE group(mm^3)

STRUCTURE	HC GROUP ($\bar{x}$ ± S)	MRIN-MTLE GROUP ($\bar{x}$ ± S)	*T*	*P*	STRUCTURE	HC GROUP ($\bar{x}$ ± S)	MRIN-MTLE GROUP ($\bar{x}$ ± S)	*T*	*P*
lh_posteriorcingulate	3089.24±602.18	2982.53±769.57	1.505	0.133	rh_lateralorbitofrontal	7298.63±1005.56	7487.2±1225.13	-1.64	0.102
lh_rostralanteriorcingulate	2462.91±588	2554.93±624.27	-1.479	0.14	rh_superiorfrontal	21406.01±3080.16	20859.43±3576.52	1.596	0.111
lh_lateraloccipital	12194.55±1928.57	12509.45±2401.67	-1.409	0.16	rh_frontalpole	1308.01±248.29	1345.36±300.82	-1.32	0.188
lh_frontalpole	1085.81±191.36	1115.11±232.8	-1.34	0.181	rh_lateraloccipital	12302.72±2055.08	12590.24±2433.11	-1.244	0.214
lh_superiorparietal	12994.68±1946.99	13217.77±2415.94	-0.991	0.322	rh_isthmuscingulate	2417.99±539.89	2339.98±680.5	1.238	0.217
lh_postcentral	9669.83±1440.19	9512.25±1710.02	0.972	0.332	rh_parsopercularis	3824.82±681.5	3728.1±877.31	1.2	0.231
lh_inferiorparietal	12161.1±1964.76	12369.44±2490.25	-0.905	0.366	rh_temporalpole	2612.39±513.18	2543.6±620.36	1.178	0.24
lh_fusiform	9293.92±1598.86	9158.71±1796.83	0.775	0.439	rh_lingual	6849.39±1455.03	6669.99±1579.06	1.152	0.25
lh_superiortemporal	12107.49±2116.36	11929.59±2610.2	0.73	0.466	rh_parsorbitalis	2815.97±454.6	2862.69±536.77	-0.916	0.36
lh_paracentral	3492.09±539.41	3450.46±657.56	0.675	0.5	rh_inferiortemporal	11080.82±1977.54	10895.41±2211.52	0.861	0.39
lh_medialorbitofrontal	5491.34±713.13	5438.64±839.54	0.66	0.51	rh_parahippocampal	1820.42±347.95	1785.32±465.93	0.832	0.406
lh_isthmuscingulate	2595.64±522.97	2552.76±743.78	0.65	0.516	rh_transversetemporal	893.38±190.95	875.91±230.66	0.804	0.422

Table2(c): Brain structure volume comparison between HC group and MRIn-MTLE group(mm^3)

STRUCTURE	HC GROUP ($\bar{x}$ ± S)	MRIN-MTLE GROUP ($\bar{x}$ ± S)	*T*	*P*	STRUCTURE	HC GROUP ($\bar{x}$ ± S)	MRIN-MTLE GROUP ($\bar{x}$ ± S)	*T*	*P*
lh_parahippocampal	2029.06±366.35	2000.52±485.73	0.647	0.518	rh_medialorbitofrontal	5748.45±790.25	5818.65±924.13	-0.796	0.427
lh_middletemporal	10771.78±2294.63	10614.79±2483.52	0.64	0.523	rh_postcentral	9309.09±1506.17	9195.62±1677.52	0.694	0.488
lh_cuneus	3083.04±611.11	3043.64±696.04	0.586	0.558	rh_rostralanteriorcingulate	1837.59±484.04	1806.03±502.96	0.623	0.533
lh_transversetemporal	1202.35±262.02	1185.7±315.95	0.559	0.576	rh_middletemporal	11815.96±2224.82	11668.03±2639.22	0.591	0.555
lh_lingual	6294.47±1366.68	6364.65±1419.69	-0.491	0.624	rh_insula	6844.95±929.87	6892.22±1095.31	-0.453	0.651
lh_temporalpole	2583.44±462.97	2559.54±542.12	0.462	0.644	rh_caudalanteriorcingulate	1869.75±562.2	1844.04±548.03	0.451	0.652
lh_entorhinal	1838.03±444.33	1859.04±499.23	-0.433	0.665	rh_paracentral	3858.65±628.27	3840.79±750.81	0.251	0.802
lh_insula	6942.18±871.65	6974.03±956.81	-0.339	0.735	rh_inferiorparietal	14711.38±2527.41	14655.93±2806.45	0.202	0.84
lh_pericalcarine	2040.12±478.37	2024.98±505.77	0.3	0.764	rh_superiorparietal	12677.07±1912.08	12642.49±2337.33	0.158	0.875
lh_parsorbitalis	2346.14±386.23	2353.33±401.58	-0.178	0.859	rh_pericalcarine	2322.37±519.65	2315.53±604.81	0.118	0.906
lh_caudalanteriorcingulate	1555.81±437.98	1550.92±518.07	0.099	0.921	rh_rostralmiddlefrontal	16001.27±2846.94	15966.83±3091.21	0.113	0.91
lh_lateralorbitofrontal	7484.83±932.26	7494.85±1072.72	-0.097	0.923	rh_superiortemporal	11557.65±2033.44	11531.66±2436.62	0.113	0.91

Table2(d): Brain structure volume comparison between HC group and MRIn-MTLE group(mm^3)

STRUCTURE	HC GROUP ($\bar{x}$ ± S)	MRIN-MTLE GROUP ($\bar{x}$ ± S)	*T*	*P*	STRUCTURE	HC GROUP ($\bar{x}$ ± S)	MRIN-MTLE GROUP ($\bar{x}$ ± S)	*T*	*P*
lh_supramarginal	11189.78±2102.32	11169.78±2477.48	0.085	0.932	rh_parstriangularis	4308.67±861.76	4310.84±982.33	-0.023	0.982
lh_precuneus	9452.32±1508.67	9446.18±1863.95	0.035	0.972	rh_supramarginal	9606.74±1872.25	9608.64±2184.23	-0.009	0.993
Brain Volume Without Ventricles	1123787.36±123038.06	1112130.07±126810.26	0.909	0.364	Estimated total intracranial volume	1469993.59±169968.81	1411306.37±198446.73	3.096	0.002

** lh= left hemisphere; ** rh=right hemisphere*

2.2. Comparison of brain subregion volume differences between male and female healthy controls

Female healthy controls eTIV was smaller than male (1399306.99±159346.34 vs 1533611.52±153933.48, *P*<0.001). 25/33 left hemisphere subregions and 21/33 right hemisphere subregions were smaller than male(*P*<0.05) (Table 3).

Table 3(a): Brain structure volume comparison between males and females in HC group (mm^3)

Structure	Female	Male	*T*	*P*	Structure	Female	Male	*T*	*P*
***lh_lateraloccipital**	11309.36±1734.54	12991.23±1744.26	-6.654	0	**rh_inferiorparietal	13941.18±2116.25	15404.57±2672.86	-4.153	0
lh_medialorbitofrontal	5200.97±589.81	5752.68±715.9	-5.76	0	rh_lateraloccipital	11468.47±1877.62	13053.55±1921.27	-5.74	0
lh_rostralmiddlefrontal	14634.34±1981.27	16465.01±2715.51	-5.344	0	rh_lateralorbitofrontal	6997.49±782.23	7569.66±1106.2	-4.147	0
lh_insula	6625.83±721.19	7226.9±900.01	-5.043	0	rh_medialorbitofrontal	5472.04±636.64	5997.21±834.2	-4.837	0
lh_parsopercularis	4306.07±736.73	4865.41±973.11	-4.493	0	rh_middletemporal	11127.3±2068.34	12435.75±2187.38	-4.224	0

Table 3(b): Brain structure volume comparison between males and females in HC group (mm^3)

lh_parstriangularis	**3424.08±541.74**	**3836.31±755.29**	**-4.354**	**0**	**rh_precuneus**	**9366.6±1367.73**	**10320.8±1862.3**	**-3.988**	**0**
lh_inferiortemporal	10853.73±1767.85	12113.04±2263.96	-4.295	0	rh_rostralanteriorcingulate	1708.4±406.81	1953.87±519.3	-3.645	0
lh_rostralanteriorcingulate	2281.73±488.02	2625.96±623.91	-4.257	0	rh_rostralmiddlefrontal	15190.54±2323.68	16730.93±3079.59	-3.858	0
lh_fusiform	8811.89±1369.82	9727.75±1670.95	-4.104	0	rh_frontalpole	1235.74±208.18	1373.05±264.02	-3.95	0
lh_middletemporal	10083.68±1978.77	11391.08±2390.42	-4.081	0	rh_insula	6572.34±770.12	7090.29±994.58	-3.981	0
lh_superiorfrontal	21504.79±2708.24	23273.74±3301.28	-4.053	0	rh_fusiform	8664.69±1323.74	9460.97±1840.73	-3.447	0.001
lh_lateralorbitofrontal	7207.86±771.71	7734.11±995.65	-4.039	0	rh_parsorbitalis	2702.77±359.23	2917.85±506.35	-3.402	0.001
lh_parsorbitalis	2236.18±333.55	2445.1±404.82	-3.857	0	rh_superiorfrontal	20656±2664.11	22081.01±3280.26	-3.3	0.001
lh_inferiorparietal	11629.47±1867.98	12639.57±1935.09	-3.652	0	rh_cuneus	3299.47±628.09	3579.75±653.83	-3.006	0.003
lh_precuneus	9077.86±1258.68	9789.33±1636.71	-3.331	0.001	rh_inferiortemporal	10630.52±1674.13	11486.08±2143.82	-3.042	0.003
lh_frontalpole	1038.5±170.31	1128.38±199.92	-3.317	0.001	rh_superiortemporal	11092.18±1723.34	11976.58±2202.2	-3.059	0.003

Table 3(c): Brain structure volume comparison between males and females in HC group (mm³)

Structure	Female	Male	*T*	*P*	Structure	Female	Male	*T*	*P*
lh_isthmuscingulate	2468.92±439.49	2709.68±566.34	-3.248	0.001	rh_lingual	6536.11±1279.53	7131.34±1549.32	-2.869	0.005
lh_cuneus	2939.39±567	3212.32±623.14	-3.145	0.002	rh_parstriangularis	4128.34±705.46	4470.97±956.12	-2.785	0.006
lh_lingual	6003.23±1259.89	6556.59±1411.51	-2.838	0.005	rh_postcentral	9028.2±1461.39	9561.9±1508.2	-2.471	0.014
lh_superiortemporal	11665.31±1929.77	12505.46±2205.72	-2.78	0.006	rh_caudalanteriorcingulate	1769.07±490.08	1960.37±608.25	-2.397	0.018
lh_posteriorcingulate	2967.89±523.5	3198.46±648.43	-2.678	0.008	rh_superiorparietal	12334.27±1620.42	12985.59±2101.48	-2.373	0.019
lh_entorhinal	1754.34±357.01	1913.34±500.23	-2.497	0.013	rh_parsopercularis	3725.13±563.15	3914.54±764.45	-1.957	0.052
lh_supramarginal	10805.41±1837.16	11535.72±2268.98	-2.421	0.016	rh_paracentral	3770.19±552.61	3938.26±682.29	-1.853	0.065
lh_postcentral	9431.94±1269.9	9883.92±1553.13	-2.181	0.03	rh_isthmuscingulate	2345.24±382.39	2483.47±644.88	-1.818	0.071
lh_caudalmiddlefrontal	6029.09±1017.42	6375.22±1349.9	-1.979	0.049	rh_entorhinal	1770.98±444.16	1883.02±539.15	-1.569	0.118
lh_precentral	13127.54±1859.83	13601.84±1829.32	-1.77	0.078	rh_posteriorcingulate	3015.63±579.26	3164.73±761.44	-1.506	0.134

Table 3(d): Brain structure volume comparison between males and females in HC group (mm^3)

Structure	Female	Male	*T*	*P*	Structure	Female	Male	*T*	*P*
lh_paracentral	3426.71±493.36	3550.93±573.83	-1.591	0.113	rh_supramarginal	9399.63±1770.86	9793.13±1949.03	-1.451	0.149
lh_pericalcarine	1986.61±461.88	2088.28±490.04	-1.467	0.144	rh_pericalcarine	2271.1±527.56	2368.51±510.67	-1.292	0.198
lh_temporalpole	2540.12±417.13	2622.42±499.53	-1.225	0.222	rh_precentral	12955.14±1874.09	13323.41±2226.76	-1.226	0.222
lh_transversetemporal	1177.96±229.12	1224.31±287.82	-1.219	0.224	rh_parahippocampal	1794.66±281.7	1843.6±398.31	-0.968	0.334
lh_superiorparietal	12894.13±1755.77	13085.18±2109.06	-0.674	0.501	rh_transversetemporal	881.28±169.03	904.27±208.98	-0.828	0.409
lh_parahippocampal	2013.28±413.96	2043.27±318.96	-0.562	0.574	rh_caudalmiddlefrontal	5979±958.6	6099.28±1548.13	-0.651	0.516
lh_caudalanteriorcingulate	1539.14±410.75	1570.8±462.67	-0.496	0.62	rh_temporalpole	2591.56±409.05	2631.14±592.95	-0.54	0.59
BrainVolumeWithoutVentricles	1073687.53±101530.98	1168877.2±123684.28	-5.76	0	EstimatedTotalIntraCranialVol	1399306.99±159346.34	1533611.52±153933.48	-5.906	0

** lh= left hemisphere; ** rh=right hemisphere*

2.3. Comparison of brain subregion volume differences between male and female MRIn-MTLE group

Female healthy controls eTIV was smaller than male (1340873.07±173887.29 vs 1474696.34±198571.91, P<0.001). 29/33 left hemisphere subregions and 28/33 right hemisphere subregions were smaller than male(P<0.05) (Table 4).

Table 4(a): Brain structure volume comparison between males and females in MRIn-MTLE group (mm^3)

STRUCTURE	FEMALE	MALE	*T*	*P*	STRUCTURE	FEMALE	MALE	*t*	*P*
lh_cuneus	2811.89±599.46	3252.21±713.5	-4.578	0	rh_fusiform	8278.91±1729.35	9224.87±1811.15	-3.672	0
lh_fusiform	8585.18±1614.02	9674.89±1803.77	-4.369	0	rh_inferiorparietal	13867.58±2204.01	15365.44±3097.71	-3.868	0
lh_inferiortemporal	10426.56±2041.82	11762.83±2360.47	-4.151	0	rh_inferiortemporal	9965.03±1893.71	11732.74±2148.96	-5.987	0
lh_isthmuscingulate	2329.27±702.42	2753.9±725.46	-4.089	0	rh_isthmuscingulate	2129.26±613.96	2529.63±684.46	-4.226	0
lh_lateraloccipital	11653.64±2192.42	13279.68±2329.26	-4.94	0	rh_lateraloccipital	11571.42±1887.17	13507.18±2511.44	-6.042	0
lh_postcentral	9031.86±1395.52	9944.61±1852.86	-3.858	0	rh_lateralorbitofrontal	7101.72±1117.48	7834.13±1219.08	-4.301	0
lh_precuneus	8899.33±1512.01	9938.35±2015.19	-4.044	0	rh_middletemporal	10708.57±2568.39	12531.54±2403.62	-5.053	0
lh_insula	6676.59±795.73	7241.72±1012.77	-4.244	0	rh_postcentral	8753.64±1421.65	9593.4±1793.87	-3.593	0
lh_entorhinal	1735.49±497.14	1970.23±476.71	-3.321	0.001	rh_insula	6575.73±988.54	7179.94±1112.83	-3.93	0
lh_lateralorbitofrontal	7228.41±878	7734.65±1175.24	-3.384	0.001	rh_cuneus	3076.84±654.93	3444.85±798.08	-3.452	0.001
lh_lingual	6012.51±1298.79	6681.58±1455.05	-3.329	0.001	rh_medialorbitofrontal	5582.57±760.21	6031.12±1007.27	-3.435	0.001
lh_pericalcarine	1899.02±435.08	2138.34±539.24	-3.381	0.001	rh_posteriorcingulate	2759.93±637.84	3099.33±689.71	-3.509	0.001

Table 4(b): Brain structure volume comparison between males and females in MRIn-MTLE group (mm^3)

STRUCTURE	FEMALE	MALE	*T*	*P*	STRUCTURE	FEMALE	MALE	*t*	*P*
lh_rostralanteriorcingulate	2394.81±543.17	2699.04±659.16	-3.449	0.001	rh_lingual	6304.64±1387.27	6998.8±1673.17	-3.093	0.002
lh_superiortemporal	11280.78±2258.52	12513.52±2773.83	-3.336	0.001	rh_temporalpole	2399.99±579.1	2672.85±630.56	-3.095	0.002
lh_supramarginal	10541.92±2120.87	11734.86±2644.47	-3.406	0.001	rh_superiortemporal	10982.01±2136.34	12026.34±2590.31	-3.012	0.003
lh_temporalpole	2418.3±561.82	2686.65±492.81	-3.507	0.001	rh_pericalcarine	2181.9±524.98	2435.8±647.85	-2.947	0.004
lh_medialorbitofrontal	5244.47±710.08	5613.39±909.48	-3.092	0.002	rh_parsorbitalis	2747.33±494.82	2966.51±554.03	-2.863	0.005
lh_middletemporal	10040.1±2346.54	11132.01±2500.89	-3.094	0.002	rh_rostralanteriorcingulate	1700.02±449.19	1901.44±531.17	-2.806	0.006
lh_parahippocampal	1894.03±443.7	2096.36±503.84	-2.924	0.004	rh_rostralmiddlefrontal	15345.51±2324.21	16526.02±3566.43	-2.728	0.007
lh_inferiorparietal	11853.74±1979.85	12833.56±2802.81	-2.804	0.006	rh_caudalanteriorcingulate	1734.06±500.62	1943.02±571.99	-2.666	0.008
lh_precentral	12385.34±2227.02	13333.19±2647.5	-2.655	0.009	rh_precuneus	9148.5±1496.96	9838.78±2029.66	-2.685	0.008
lh_superiorparietal	12755.81±1985.84	13633.54±2688.69	-2.576	0.011	rh_transversetemporal	830.28±221.07	916.97±232.46	-2.627	0.009

Table 4(c): Brain structure volume comparison between males and females in MRIn-MTLE group (mm^3)

STRUCTURE	FEMALE	MALE	*T*	*P*	STRUCTURE	FEMALE	MALE	*t*	*P*
lh_parstriangularis	3398.57±579.82	3642.22±742.3	-2.502	0.013	rh_caudalmiddlefrontal	5441.88±1113.23	5917.05±1410.94	-2.558	0.011
lh_transversetemporal	1128.67±270.37	1237.03±345.31	-2.42	0.016	rh_parsopercularis	3562.44±765.9	3877.19±945.85	-2.503	0.013
lh_posteriorcingulate	2842.04±795.01	3108.97±726.88	-2.418	0.017	rh_parstriangularis	4127.79±935.57	4475.59±998.73	-2.469	0.014
lh_superiorfrontal	20956.86±3295.47	22175.79±3854.62	-2.33	0.021	rh_precentral	12178.48±2156.11	12972.05±2344.52	-2.42	0.016
lh_rostralmiddlefrontal	14699.38±1909.21	15469.06±3124.56	-2.071	0.04	rh_entorhinal	1644.94±360.07	1787.55±558.96	-2.111	0.036
lh_caudalanteriorcingulate	1470.83±490.64	1622.99±533.76	-2.038	0.043	rh_parahippocampal	1711.06±385.98	1852.15±520.56	-2.103	0.037
lh_caudalmiddlefrontal	5585.6±1056.4	5949.72±1392.88	-2.013	0.046	rh_superiorfrontal	20354.34±3221.42	21314.01±3827.55	-1.859	0.065
lh_parsopercularis	4233.1±845.92	4483.58±1001.43	-1.852	0.066	rh_supramarginal	9313.26±2030.78	9874.48±2291.24	-1.779	0.077
lh_paracentral	3385.7±599.66	3508.75±703.52	-1.29	0.199	rh_frontalpole	1310.51±294.25	1376.73±304.68	-1.52	0.13
lh_frontalpole	1092.61±254.35	1135.36±210.78	-1.266	0.207	rh_paracentral	3774.6±865.33	3900.37±628.84	-1.154	0.25

Table 4(d): Brain structure volume comparison between males and females in MRIn-MTLE group (mm^3)

STRUCTURE	FEMALE	MALE	*T*	*P*	STRUCTURE	FEMALE	MALE	*t*	*P*
lh_parsorbitalis	2334.27±365.08	2370.49±432.93	-0.62	0.536	rh_superiorparietal	12555.27±2045.07	12720.99±2580.03	-0.493	0.623
BrainVolumeWithoutVentricles	1067605.02±101117.49	1152202.61±134475.15	-4.93	0	EstimatedTotalIntraCranialVol	1340873.07±173887.29	1474696.34±198571.91	-4.918	0

2.4 Comparison of male differences in brain subregion volume between the groups

The eTIV and volumes of left pars opercularis gyrus, left rostral middle frontal gyrus, left caudal middle frontal gyrus, left superior frontal gyrus were larger in HC group than in MRIn-MTLE group (*P*<0.05), differences of the other brain structure volumes between two groups were statistically insignificant(*P*>0.05) (Table 5; Figure 1A).

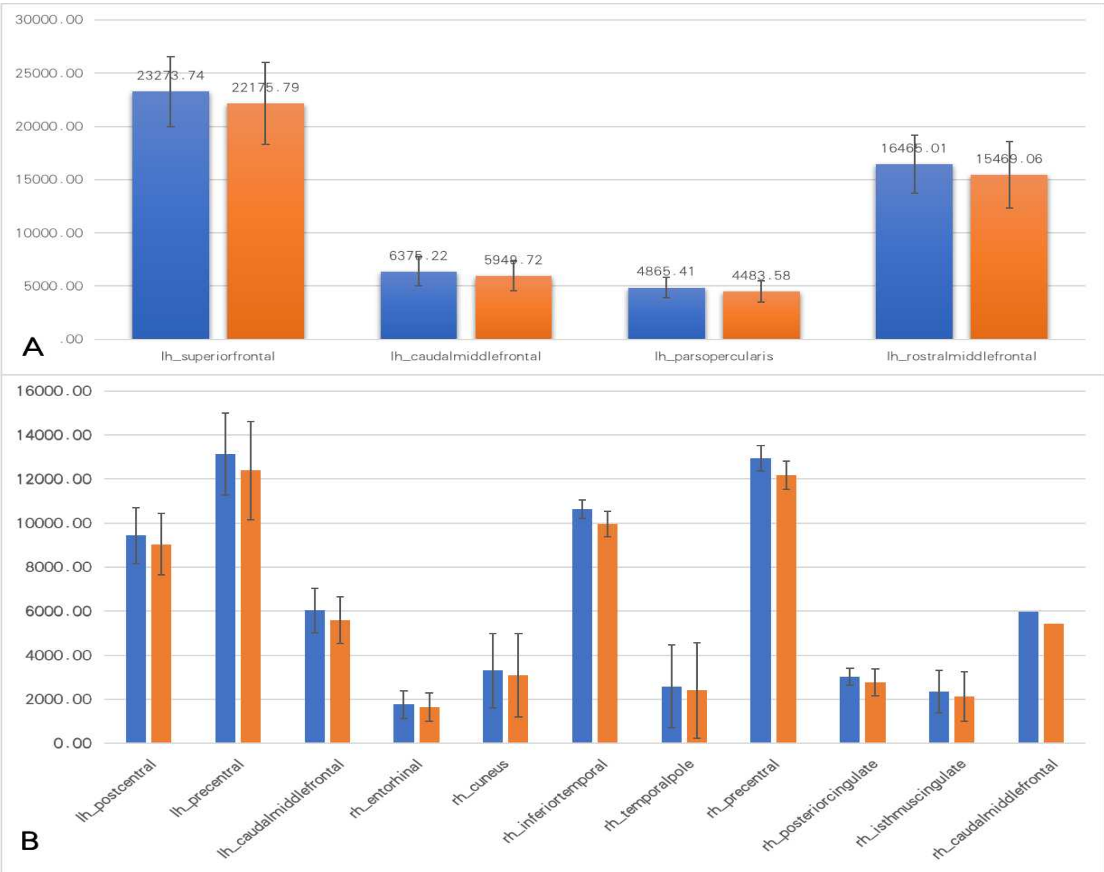

Figure 1: Differences in brain region volumes in the two groups: A) in males; B) in females (mm^3)

Table 5: Brain structure volume comparison between males in HC group and MRIn-MTLE group(mm^3)

STRUCTURE	HC GROUP ($\bar{x}$ ± S)	MRIN-MTLE GROUP ($\bar{x}$ ± S)	*T*	*P*	STRUCTURE	HC GROUP ($\bar{x}$ ± S)	MRIN-MTLE GROUP ($\bar{x}$ ± S)	*T*	*P*
***lh_parsopercularis**	4865.41±973.11	4483.58±1001.43	2.734	0.007	**rh_precuneus	10320.8±1862.3	9838.78±2029.66	1.75	0.082
lh_rostralmiddlefrontal	16465.01±2715.51	15469.06±3124.56	2.406	0.017	rh_lateralorbitofrontal	7569.66±1106.2	7834.13±1219.08	-1.607	0.11
lh_caudalmiddlefrontal	6375.22±1349.9	5949.72±1392.88	2.194	0.029	rh_superiorfrontal	22081.01±3280.26	21314.01±3827.55	1.522	0.13
lh_superiorfrontal	23273.74±3301.28	22175.79±3854.62	2.163	0.032	rh_lateraloccipital	13053.55±1921.27	13507.18±2511.44	-1.435	0.153
lh_parstriangularis	3836.31±755.29	3642.22±742.3	1.833	0.068	rh_cuneus	3579.75±653.83	3444.85±798.08	1.308	0.193
lh_superiorparietal	13085.18±2109.06	13633.54±2688.69	-1.605	0.11	rh_entorhinal	1883.02±539.15	1787.55±558.96	1.229	0.22
lh_parsorbitalis	2445.1±404.82	2370.49±432.93	1.259	0.21	rh_precentral	13323.41±2226.76	12972.05±2344.52	1.087	0.279
lh_medialorbitofrontal	5752.68±715.9	5613.39±909.48	1.203	0.23	rh_fusiform	9460.97±1840.73	9224.87±1811.15	0.914	0.362
lh_inferiortemporal	12113.04±2263.96	11762.83±2360.47	1.071	0.286	rh_caudalmiddlefrontal	6099.28±1548.13	5917.05±1410.94	0.87	0.385

Table 5(b): Brain structure volume comparison between males in HC group and MRIn-MTLE group(mm^3)

STRUCTURE	HC GROUP ($\bar{x}$ ± S)	MRIN-MTLE GROUP ($\bar{x}$ ± S)	*T*	*P*	STRUCTURE	HC GROUP ($\bar{x}$ ± S)	MRIN-MTLE GROUP ($\bar{x}$ ± S)	*T*	*P*
lh_lateraloccipital	12991.23±1744.26	13279.68±2329.26	-0.991	0.323	rh_pericalcarine	2368.51±510.67	2435.8±647.85	-0.816	0.416
lh_posteriorcingulate	3198.46±648.43	3108.97±726.88	0.919	0.359	rh_inferiortemporal	11486.08±2143.82	11732.74±2148.96	-0.813	0.417
lh_temporalpole	2622.42±499.53	2686.65±492.81	-0.915	0.361	rh_superiorparietal	12985.59±2101.48	12720.99±2580.03	0.795	0.428
lh_parahippocampal	2043.27±318.96	2096.36±503.84	-0.89	0.375	rh_rostralanteriorcingulate	1953.87±519.3	1901.44±531.17	0.706	0.481
lh_precentral	13601.84±1829.32	13333.19±2647.5	0.835	0.405	rh_parsorbitalis	2917.85±506.35	2966.51±554.03	-0.648	0.518
lh_entorhinal	1913.34±500.23	1970.23±476.71	-0.823	0.411	rh_posteriorcingulate	3164.73±761.44	3099.33±689.71	0.637	0.525
lh_rostralanteriorcingulate	2625.96±623.91	2699.04±659.16	-0.805	0.422	rh_insula	7090.29±994.58	7179.94±1112.83	-0.599	0.55
lh_middletemporal	11391.08±2390.42	11132.01±2500.89	0.749	0.455	rh_lingual	7131.34±1549.32	6998.8±1673.17	0.581	0.562

Table 5(c): Brain structure volume comparison between males in HC group and MRIn-MTLE group(mm^3)

STRUCTURE	HC GROUP ($\bar{x}$ ± S)	MRIN-MTLE GROUP ($\bar{x}$ ± S)	*T*	*P*	STRUCTURE	HC GROUP ($\bar{x}$ ± S)	MRIN-MTLE GROUP ($\bar{x}$ ± S)	*T*	*P*
lh_caudalanteriorcingulate	1570.8±462.67	1622.99±533.76	-0.739	0.461	rh_isthmuscingulate	2483.47±644.88	2529.63±684.46	-0.491	0.624
lh_pericalcarine	2088.28±490.04	2138.34±539.24	-0.687	0.493	rh_temporalpole	2631.14±592.95	2672.85±630.56	-0.482	0.63
lh_lingual	6556.59±1411.51	6681.58±1455.05	-0.617	0.538	rh_rostralmiddlefrontal	16730.93±3079.59	16526.02±3566.43	0.435	0.664
lh_precuneus	9789.33±1636.71	9938.35±2015.19	-0.574	0.567	rh_paracentral	3938.26±682.29	3900.37±628.84	0.408	0.683
lh_supramarginal	11535.72±2268.98	11734.86±2644.47	-0.572	0.568	rh_transversetemporal	904.27±208.98	916.97±232.46	-0.406	0.685
lh_inferiorparietal	12639.57±1935.09	12833.56±2802.81	-0.57	0.57	rh_parsopercularis	3914.54±764.45	3877.19±945.85	0.307	0.759
lh_isthmuscingulate	2709.68±566.34	2753.9±725.46	-0.48	0.631	rh_middletemporal	12435.75±2187.38	12531.54±2403.62	-0.295	0.768
lh_paracentral	3550.93±573.83	3508.75±703.52	0.465	0.643	rh_supramarginal	9793.13±1949.03	9874.48±2291.24	-0.27	0.787

Table 5(d): Brain structure volume comparison between males in HC group and MRIn-MTLE group(mm^3)

STRUCTURE	HC GROUP ($\bar{x}$ ± S)	MRIN-MTLE GROUP ($\bar{x}$ ± S)	*T*	*P*	STRUCTURE	HC GROUP ($\bar{x}$ ± S)	MRIN-MTLE GROUP ($\bar{x}$ ± S)	*T*	*P*
lh_cuneus	3212.32±623.14	3252.21±713.5	-0.421	0.674	rh_medialorbitofrontal	5997.21±834.2	6031.12±1007.27	-0.259	0.796
lh_transversetemporal	1224.31±287.82	1237.03±345.31	-0.283	0.778	rh_caudalanteriorcingulate	1960.37±608.25	1943.02±571.99	0.208	0.836
lh_postcentral	9883.92±1553.13	9944.61±1852.86	-0.251	0.802	rh_superiortemporal	11976.58±2202.2	12026.34±2590.31	-0.146	0.884
lh_frontalpole	1128.38±199.92	1135.36±210.78	-0.24	0.81	rh_postcentral	9561.9±1508.2	9593.4±1793.87	-0.134	0.893
lh_fusiform	9727.75±1670.95	9674.89±1803.77	0.215	0.83	rh_parahippocampal	1843.6±398.31	1852.15±520.56	-0.13	0.896
lh_insula	7226.9±900.01	7241.72±1012.77	-0.109	0.913	rh_inferiorparietal	15404.57±2672.86	15365.44±3097.71	0.096	0.924
lh_superiortemporal	12505.46±2205.72	12513.52±2773.83	-0.023	0.982	rh_frontalpole	1373.05±264.02	1376.73±304.68	-0.091	0.927
lh_lateralorbitofrontal	7734.11±995.65	7734.65±1175.24	-0.004	0.997	rh_parstriangularis	4470.97±956.12	4475.59±998.73	-0.033	0.973

Table 5(e): Brain structure volume comparison between males in HC group and MRIn-MTLE group(mm^3)

STRUCTURE	HC GROUP ($\bar{x}$ ± S)	MRIN-MTLE GROUP ($\bar{x}$ ± S)	*T*	*P*	STRUCTURE	HC GROUP ($\bar{x}$ ± S)	MRIN-MTLE GROUP ($\bar{x}$ ± S)	*T*	*P*
BrainVolumeWithout Ventricles	1168877.2±123684.28	1152202.61±134475.15	0.913	0.363	Estimated total intracranial volume	1533611.52±153933.48	1474696.34±198571.91	2.345	0.02

** lh= left hemisphere; ** rh=right hemisphere*

2.5. Comparison of female differences in brain subregion volume between the groups

The eTIV and volumes of left caudal middle frontal gyrus, left precentral gyrus, left postcentral gyrus, right caudal middle frontal gyrus, right isthmus of cingulate gyrus, right posterior cingulate gyrus, right precentral gyrus, right temporal pole, right inferior temporal gyrus, right cuneus, right entorhinal cortex were larger in HC group than in MRIn-MTLE group, (P<0.05), differences of the other brain structure volumes between two groups were statistically insignificant(P>0.05) (Table 6, Figure 1B).

Table 6(a): Brain structure volume comparison between females in HC group and MRIn-MTLE group(mm^3)

STRUCTURE	HC GROUP	MRIN-MTLE GROUP	T	P	STRUCTURE	HC GROUP	MRIN-MTLE GROUP	T	P
lh_caudalmiddlefrontal	6029.09±1017.42	5585.6±1056.4	2.869	0.005	**rh_caudalmiddlefrontal**	5979±958.6	5441.88±1113.23	3.469	0.001
lh_precentral	13127.54±1859.83	12385.34±2227.02	2.427	0.016	rh_isthmuscingulate	2345.24±382.39	2129.26±613.96	2.833	0.005
lh_postcentral	9431.94±1269.9	9031.86±1395.52	2.012	0.046	rh_posteriorcingulate	3015.63±579.26	2759.93±637.84	2.815	0.005
lh_parsorbitalis	2236.18±333.55	2334.27±365.08	-1.882	0.061	rh_precentral	12955.14±1874.09	12178.48±2156.11	2.579	0.011

Table 6(b): Brain structure volume comparison between females in HC group and MRIn-MTLE group(mm^3)

STRUCTURE	HC GROUP	MRIN-MTLE GROUP	T	P	STRUCTURE	HC GROUP	MRIN-MTLE GROUP	T	P
lh_parahippocampal	2013.28±413.96	1894.03±443.7	1.864	0.064	rh_temporalpole	2591.56±409.05	2399.99±579.1	2.563	0.011
lh_frontalpole	1038.5±170.31	1092.61±254.35	-1.677	0.096	rh_inferiortemporal	10630.52±1674.13	9965.03±1893.71	2.498	0.013
lh_temporalpole	2540.12±417.13	2418.3±561.82	1.652	0.101	rh_cuneus	3299.47±628.09	3076.84±654.93	2.327	0.021
lh_isthmuscingulate	2468.92±439.49	2329.27±702.42	1.599	0.112	rh_entorhinal	1770.98±444.16	1644.94±360.07	2.091	0.038
lh_inferiortemporal	10853.73±1767.85	10426.56±2041.82	1.501	0.135	rh_frontalpole	1235.74±208.18	1310.51±294.25	-1.968	0.051
lh_cuneus	2939.39±567	2811.89±599.46	1.466	0.144	rh_transversetemporal	881.28±169.03	830.28±221.07	1.739	0.084
lh_rostralanteriorcingulate	2281.73±488.02	2394.81±543.17	-1.469	0.144	rh_fusiform	8664.69±1323.74	8278.91±1729.35	1.68	0.095
lh_transversetemporal	1177.96±229.12	1128.67±270.37	1.319	0.189	rh_parahippocampal	1794.66±281.7	1711.06±385.98	1.66	0.099
lh_pericalcarine	1986.61±461.88	1899.02±435.08	1.31	0.192	rh_parsopercularis	3725.13±563.15	3562.44±765.9	1.624	0.106

Table 6(c): Brain structure volume comparison between females in HC group and MRIn-MTLE group(mm^3)

STRUCTURE	HC GROUP	MRIN-MTLE GROUP	T	P	STRUCTURE	HC GROUP	MRIN-MTLE GROUP	T	P
lh_posteriorcingulate	2967.89±523.5	2842.04±795.01	1.254	0.2111	rh_postcentral	9028.2±1461.39	8753.64±1421.65	1.278	0.2003
lh_superiortemporal	11665.31±1929.77	11280.78±2258.52	1.228	0.2221	rh_middletemporal	11127.3±2068.34	10708.57±2568.39	1.205	0.233
lh_superiorfrontal	21504.79±2708.24	20956.86±3295.47	1.219	0.2225	rh_lingual	6536.11±1279.53	6304.64±1387.27	1.164	0.2446
lh_lateraloccipital	11309.36±1734.54	11653.64±2192.42	-1.168	0.244	rh_pericalcarine	2271.1±527.56	2181.9±524.98	1.137	0.2257
lh_fusiform	8811.89±1369.82	8585.18±1614.02	1.016	0.311	rh_medialorbitofrontal	5472.04±636.64	5582.57±760.21	-1.057	0.292
lh_caudalanteriorcingulate	1539.14±410.75	1470.83±490.64	1.013	0.313	rh_precuneus	9366.6±1367.73	9148.5±1496.96	1.02	0.309
lh_supramarginal	10805.41±1837.16	10541.92±2120.87	0.891	0.374	rh_superiorparietal	12334.27±1620.42	12555.27±2045.07	-0.804	0.423
lh_precuneus	9077.86±1258.68	8899.33±1512.01	0.861	0.39	rh_lateralorbitofrontal	6997.49±782.23	7101.72±1117.48	-0.725	0.47
lh_inferiorparietal	11629.47±1867.98	11853.74±1979.85	-0.782	0.435	rh_parsorbitalis	2702.77±359.23	2747.33±494.82	-0.691	0.49

Table 6(d): Brain structure volume comparison between females in HC group and MRIn-MTLE group(mm^3)

STRUCTURE	HC GROUP	MRIN-MTLE GROUP	T	P	STRUCTURE	HC GROUP	MRIN-MTLE GROUP	T	P
lh_parsopercularis	4306.07±736.73	4233.1±845.92	0.617	0.538	rh_superiorfrontal	20656±2664.11	20354.34±3221.42	0.685	0.495
lh_paracentral	3426.71±493.36	3385.7±599.66	0.501	0.617	rh_caudalanteriorcingulate	1769.07±490.08	1734.06±500.62	0.474	0.636
lh_superiorparietal	12894.13±1755.77	12755.81±1985.84	0.495	0.621	rh_rostralmiddlefrontal	15190.54±2323.68	15345.51±2324.21	-0.447	0.655
lh_insula	6625.83±721.19	6676.59±795.73	-0.448	0.654	rh_superiortemporal	11092.18±1723.34	10982.01±2136.34	0.381	0.704
lh_medialorbitofrontal	5200.97±589.81	5244.47±710.08	-0.447	0.655	rh_lateraloccipital	11468.47±1877.62	11571.42±1887.17	-0.367	0.714
lh_parstriangularis	3424.08±541.74	3398.57±579.82	0.305	0.761	rh_supramarginal	9399.63±1770.86	9313.26±2030.78	0.304	0.761
lh_entorhinal	1754.34±357.01	1735.49±497.14	0.292	0.77	rh_inferiorparietal	13941.18±2116.25	13867.58±2204.01	0.229	0.82
lh_rostralmiddlefrontal	14634.34±1981.27	14699.38±1909.21	-0.224	0.823	rh_rostralanteriorcingulate	1708.4±406.81	1700.02±449.19	0.131	0.896
lh_lateralorbitofrontal	7207.86±771.71	7228.41±878	-0.167	0.868	rh_paracentral	3770.19±552.61	3774.6±865.33	-0.041	0.968
lh_middletemporal	10083.68±1978.77	10040.1±2346.54	0.135	0.893	rh_insula	6572.34±770.12	6575.73±988.54	-0.026	0.98
lh_lingual	6003.23±1259.89	6012.51±1298.79	-0.049	0.961	rh_parstriangularis	4128.34±705.46	4127.79±935.57	0.004	0.996

Table 6(e): Brain structure volume comparison between females in HC group and MRIn-MTLE group(mm^3)

STRUCTURE	HC GROUP	MRIN-MTLE GROUP	T	P	STRUCTURE	HC GROUP	MRIN-MTLE GROUP	T	P
BrainVolumeWithoutVentricles	1073687.53±101530.98	1067605.02±101117.49	0.403	0.688	Estimated total intracranial volume	1399306.99±159346.34	1340873.07±173887.29	2.35	0.02

** lh= left hemisphere; ** rh=right hemisphere*

2.6. Effectiveness of volumetric feature-based diagnostic classification

2.6.1 Classification effectiveness of brain volume as classification features in all participants

On the validation dataset, the SVM model based on 46 features screened by RFE achieved the greatest AUC out of 3 classifiers employed. The AUC in the training dataset reached 0.780. In this point, the AUC and the accuracy of the model in test dataset approached 0.780 and 0.721, respectively (Table 7, Table 8, Figure 2).

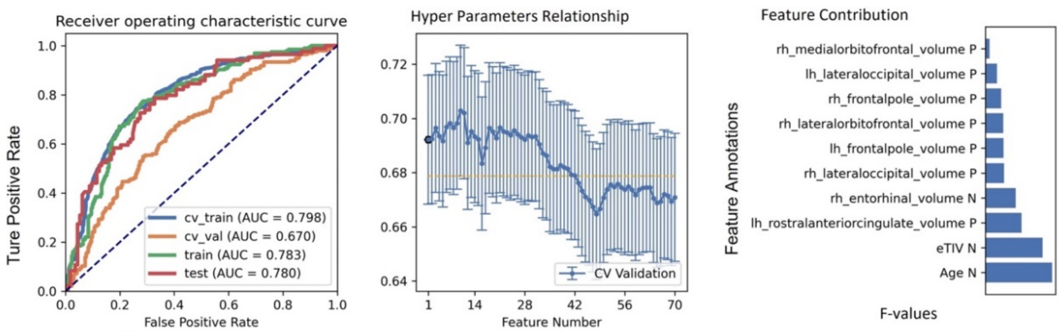

cv_val: cross validation, rh: right hemisphere, lh: left hemisphere, eTIV: estimated total intracranial volume

Figure 2: Classification efficacy of the model constructed on brain volume features in all participants

Table 7: Statistics of support vector machine model in all participants' volumetric features

STATISTICS	VALUE
ACCURACY	0.721
***AUC**	0.781
AUC 95% CIS	[0.711-0.849]
****NPV**	0.809
*****PPV**	0.641
SENSITIVITY	0.786
SPECIFICITY	0.673

**AUC: Area Under Curve, **NPV: Negative Predictive Value, ***PPV: Positive Predictive Value*

Table 8: Feature coefficients in the classification model based on all participants' brain volumes

FEATURES	INDEX	FEATURES	INDEX
Age	-3.519	lh_supramarginal_volume	0.934
*lh_caudalanteriorcingulate_volume	0.452	lh_frontalpole_volume	1.173
lh_caudalmiddlefrontal_volume	-0.781	lh_temporalpole_volume	-0.177
lh_cuneus_volume	0.639	lh_insula_volume	0.403
lh_entorhinal_volume	0.314	**eTIV	-0.821
lh_inferiorparietal_volume	0.348	rh_cuneus_volume	-1.028
lh_inferiortemporal_volume	-1.199	***rh_entorhinal_volume	-1.077
lh_isthmuscingulate_volume	-0.344	rh_inferiorparietal_volume	-0.27
lh_lateraloccipital_volume	1.116	rh_inferiortemporal_volume	0.832
lh_lateralorbitofrontal_volume	0.017	rh_lateraloccipital_volume	1.157
lh_lingual_volume	0.721	rh_lateralorbitofrontal_volume	1.189
lh_middletemporal_volume	0.888	rh_lingual_volume	-0.409
lh_paracentral_volume	0.649	rh_medialorbitofrontal_volume	0.822
lh_parsopercularis_volume	-0.933	rh_parahippocampal_volume	0.618
lh_parsorbitalis_volume	-0.684	rh_paracentral_volume	0.082
lh_parstriangularis_volume	-1.288	rh_parsorbitalis_volume	-0.106
lh_pericalcarine_volume	-0.462	rh_parstriangularis_volume	-0.058
lh_postcentral_volume	-0.173	rh_posteriorcingulate_volume	-1.418
lh_precentral_volume	-1.257	rh_precuneus_volume	-1.73
lh_precuneus_volume	0.912	rh_superiorparietal_volume	0.055
lh_rostralanteriorcingulate_volume	1.206	rh_supramarginal_volume	0.903
lh_rostralmiddlefrontal_volume	-1.527	rh_frontalpole_volume	1.226
lh_superiorparietal_volume	-0.233	rh_temporalpole_volume	-0.56

**lh: left hemisphere, **eTIV: estimated total intracranial volume, ***rh: right hemisphere*

2.6.2. Classification effectiveness of brain volume as classification features in male participants

On the validation dataset, the logistic regression model based on the nine features screened by RFE achieved the greatest AUC out of 3 classifiers employed. The AUC in the training dataset reached 0.813. In this point, the AUC and accuracy of the model in test dataset approached 0.716 and 0.700, respectively (Table 9, Table 10, Figure 3). On the test dataset, the AUC is reported to be approximately 0.716, and the accuracy is approximately 0.700. These metrics indicate how well the model generalizes to unseen data.

An AUC of 0.716 and an accuracy of 0.700 suggest that the model maintains good discriminatory power and performs reasonably well on the test data, although the performance may not be as strong as on the training data.

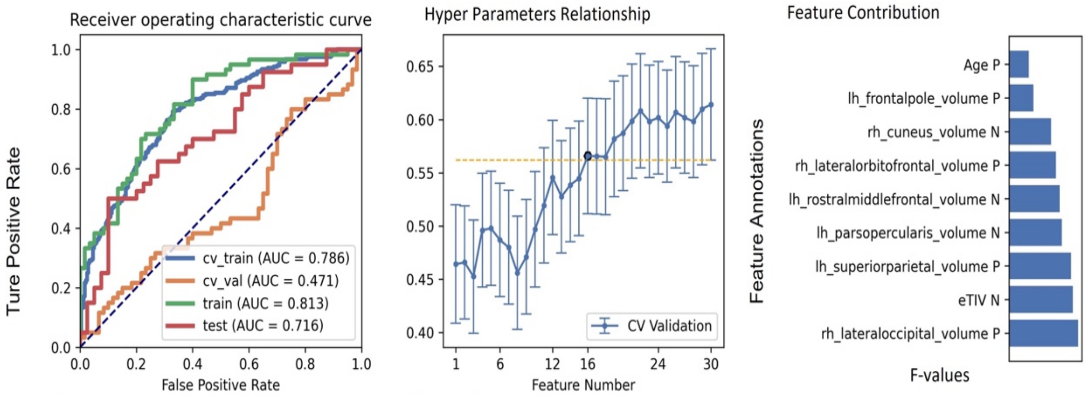

cv_val: cross validation, rh: right hemisphere, lh: left hemisphere, eTIV: estimated total intracranial volume

Figure 3: Classification efficacy of the model constructed on brain volume features in male participants

Table 9: Statistics of logistic regression model in male participants' volumetric features

Statistics	Value
Accuracy	0.7
***Auc**	0.716
Auc 95% CIs	[0.598-0.824]
****Npv**	0.643
*****Ppv**	0.833
Sensitivity	0.5
Specificity	0.9

**AUC: Area Under Curve, **NPV: Negative Predictive Value, ***PPV: Positive Predictive Value*

Table 10: Feature coefficients in the classification model based on male participants' brain volumes

FEATURES	INDEX
Age	1.591
***lh_parsopercularis_volume**	-4.274
lh_rostralmiddlefrontal_volume	-4.087
lh_superiorparietal_volume	4.999
lh_frontalpole_volume	1.968
****eTIV**	-5.166
*****rh_cuneus_volume**	-3.407
rh_lateraloccipital_volume	5.588
rh_lateralorbitofrontal_volume	3.8

**lh: left hemisphere, **eTIV: estimated total intracranial volume, ***rh: right hemisphere*

2.6.3. Classification effectiveness of brain volume as classification features in female participant

On the validation dataset, the random forest model with 30 features screened by RFE had the greatest AUC out of 3 classifiers employed. The AUC in the training dataset reached 1.000. In this point, the AUC and accuracy of the model in test dataset approached 0.761 and 0.736, respectively (Table 11, Table 12, Figure 4).

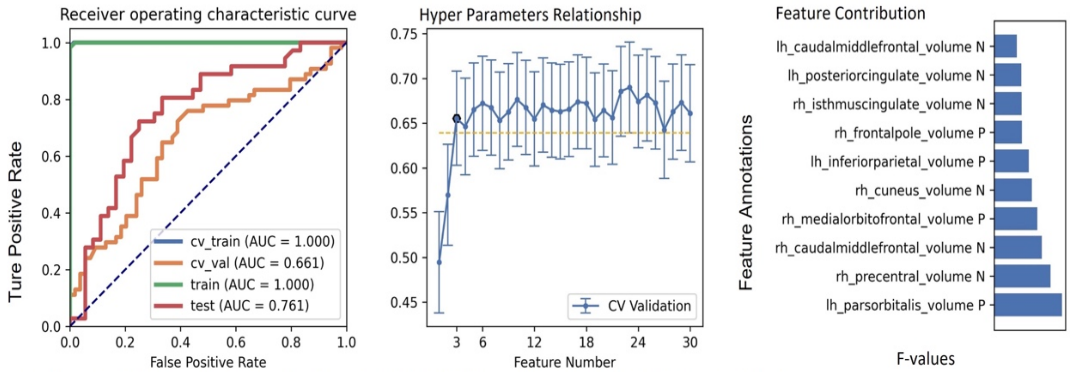

cv_val: cross validation, rh: right hemisphere, lh: left hemisphere, eTIV: estimated total intracranial volume

Figure 4: Classification efficacy of the model constructed on brain volume features in female participants

Table 11: Statistics of random forest model in female participants' volumetric features

STATISTICS	VALUE
Accuracy	0.7361
***AUC**	0.761
AUC 95% CIs	[0.648-0.868]
****NPV**	0.730
*****PPV**	0.743
Sensitivity	0.722
Specificity	0.75

**AUC: Area Under Curve, **NPV: Negative Predictive Value, ***PPV: Positive Predictive Value*

Table12(a): Ranking of features in classification model based on female participants' brain volumes

Features	Rank	Features	Rank
Age	1	rh_cuneus_volume	16
***lh_caudalanteriorcingulate_volume**	2	rh_entorhinal_volume	17
lh_caudalmiddlefrontal_volume	3	rh_inferiorparietal_volume	18
lh_cuneus_volume	4	rh_inferiortemporal_volume	19
lh_inferiorparietal_volume	5	rh_isthmuscingulate_volume	20

Table12(b): Ranking of features in classification model based on female participants' brain volumes

Features	Rank	Features	Rank
lh_inferiortemporal_volume	6	rh_lateralorbitofrontal_volume	21
lh_isthmuscingulate_volume	7	rh_medialorbitofrontal_volume	22
lh_lateraloccipital_volume	8	rh_middletemporal_volume	23
lh_parsorbitalis_volume	9	rh_postcentral_volume	24
lh_posteriorcingulate_volume	10	rh_posteriorcingulate_volume	25
lh_precentral_volume	11	rh_precentral_volume	26
lh_rostralanteriorcingulate_volume	12	rh rostral anterior cingulate_volume	27
lh_rostralmiddlefrontal_volume	13	rh rostral middle frontal volume	28
lh_transversetemporal_volume	14	rh superior temporal volume	29
****rh_caudal middle frontal volume**	15	rh frontal pole volume	30

**lh: left hemisphere, ** rh: right hemisphere*

3. Discussion

TLE is the most prevalent form of drug-resistant chronic epilepsy[5]. Targeted resection procedures, such as selective amygdala resection, are presently regarded as successful surgical approaches, with up to 80% of patients no longer experiencing seizures two years after surgery (Morris, 2006; Natsume, Bernasconi, Andermann, & Bernasconi, 2003). To determine the extent of the MTLE surgery and prognosis, the precise preoperative localization and identification of the epileptogenic focus is highly important. Many recent findings have found the use of accurate brain structure image segmentation and volume calculation to be of great value in preoperative evaluation, and as technology has advanced, the diagnostic accuracy of this technique has grown very much closer to postoperative pathological findings (Sämann et al., 2022). Which provides a noninvasive pre-operative evaluation method to improve surgical outcome and patients' symptoms (Pardoe, Berg, & Jackson, 2013).

Structural MRI provides physiologically valid and objective imaging markers and high reliability; it is thus an objective framework for investigating disease progression. This approach is also more sensitive to gray matter atrophy than visual examination. According to a 2020 review on FreeSurfer hippocampal segmentation methods and applications (Song et al., 2020), previous volumetric research has focused primarily on neurodegenerative conditions, such as AD, and less on epilepsy. We reviewed the literature on volumetric research but found that only 10 (6.2%) of the 162 identified records were epilepsy related. To fully understand the brain regions involved in MRIn-MTLE, the present study conducted structural MRI with healthy adults and epileptic patients. We then segmented and measured the telencephalic volumes of healthy adults and MRIn-MTLE patients using FreeSurfer software to obtain volume parameters of brain tissue and its subregions with high confidence.

Differences among brain regions in the left and right hemispheres were found in both the HC and MRIn-MTLE groups, suggesting that MRIn-MTLE, despite causing changes in brain region volumes, may be misdiagnosed due to the extent of physiological variability when comparing the volumes of patients' brain regions. Moreover, as neuroimaging methods advance, there is growing evidence that epilepsy is a network illness and that focal epilepsy generalizes to networks other than the epileptogenic focus[14]. In the present study, patients with MRIn-MTLE showed a reduction in the volume of several brain regions, including the temporal lobe; these results are consistent with the literature describing gray matter atrophy in patients with focal epilepsy that also occurs outside the presumed epileptogenic focus (Stefanits et al., 2017). Female MRIn-MTLE patients exhibited changes in volume in the temporal lobe, a portion of the cingulate gyrus, and frontal areas. In contrast, male MRIn-MTLE patients exhibited changes in volume in the frontal, temporal, and cingulate regions.

In the past, less emphasis has been placed on examining sex differences in the effects of MRIn-MTLE on brain structure. Similar alterations have been found in terms of cortical thickness and cortical surface area. To understand these sex related differences, a large number of neuropathological studies are required to characterize the various patterns of neuronal cell loss in the temporal lobe and adjacent temporal lobe structures in surgical specimens (Steve et al., 2020; Thom, 2014) or autopsy brains of epileptic patients. Therefore, the efficacy of imaging and neuropathological categorization methods for distinguishing the pathological forms of TLE in patients of different sexes should be evaluated.

Statistical analysis revealed several brain subregion volumes is smaller in MRIn-MTLE patients. Feature selection results came with features positively or negatively related with the MRIn-MTLE classification, 10 most discriminative features were selected (Figure2, Figure 3). In male participants, the statistical results revealed 12 differences between two groups, within which left rostral middle frontal gyrus was negatively related with classification (1 out of 10 most discriminative features).In female participants, the statistical results revealed 5 differences between two groups, within which left caudal middle frontal gyrus, right caudal middle frontal gyrus, right isthmus of cingulate gyrus, right precentral gyrus, right cuneus were negatively related with classification (5 out of 10 most discriminative features). It should be mentioned that some research have shown that sodium valproate can cause a decrease in parietal cortex thickness and volume (Tondelli, Vaudano, Sisodiya, & Meletti, 2020; Varho, Komu, Sonninen, Lähdetie, & Holopainen, 2005). The patients in the current study used carbamazepine and sodium valproate (carbamazepine N=197, sodium valproate N=23, and the combination of the two drugs N=59), and due to insufficient sample size, a comparative analysis of brain volumes in patients using sodium valproate was not performed separately in this study, but given that some participants also had a reduction in parietal volume, the effect of the drugs should be considered when making the diagnosis (Wiebe, Blume, Girvin, & Eliasziw, 2001).

Machine learning techniques can improve MRIn-MTLE lesion identification accuracy. Previous neuroimaging studies have used image histology to perform tasks such as tumor grading. Furthermore, one of the main focuses of the machine learning field in recent years has been the development of classification models for neurological diseases without obvious lesions (e.g., Alzheimer's disease and Parkinson's disease) using intrinsic features of brain tissue, and several models have been shown to have good classification efficacy, and the results of these studies have provided valuable information. The findings of these studies can be used to develop classification models based on MRIn-MTLE patient image features, in our case, there were differences between feature selection and statistical results, indicating that only revealing the differences by utilizing univariate analysis was not sufficient for feature selection, multivariate analysis, such as the machine-learning algorithm employed, provided much better effectiveness and classified the features in positive or negative, which is much clearer than statistic outcome alone (Wu et al., 2005).

This study demonstrates that brain volume as a classification feature can be utilized to diagnose and categorize MRIn-MTLE using a whole-brain volume-based classification model. The classification accuracy in the test dataset of male participants was statistically acceptable, but overfitting due to the small sample size (200 male participants and 180 female participants) limited the possibility of the classification models, which required further evaluation by increasing the sample sizes. These findings demonstrated that using structural characteristics as classification features aids in training classification models. In future studies, we would increase the sample size, divide patients into subgroups based on medication usage, and introduce novel network models to improve classification accuracy that meets clinical diagnosis needs.

4. Conclusion

This investigation sheds light on the alterations in brain volumes associated with Magnetic Resonance-Negative Temporal Lobe Epilepsy (MRIn-MTLE) among athletes and fitness enthusiasts. Epilepsy is a condition that affects individuals across various walks of life, including those actively engaged in sports and fitness activities. For a subset of these individuals, MRIn-MTLE presents a unique challenge as it lacks specific epileptogenic foci that can be identified through traditional neuroimaging techniques.

Through the utilization of T1-weighted magnetization prepared rapid gradient echo imaging (T1W-MPRAGE) scans and FreeSurfer software, we conducted a comprehensive analysis of brain regions and structures in MRIn-MTLE patients within the athlete and fitness enthusiast demographic, comparing them to a control group of healthy individuals. This investigation aimed to provide precise structural data on brain regions and assess differences in brain structure between the two groups.

The results of this study have not only deepened our understanding of MRIn-MTLE but also emphasized the need for tailored diagnostic and therapeutic approaches for athletes and fitness enthusiasts facing this condition. While conventional MRI scans may not reveal epileptogenic foci, automated segmentation tools and volumetric parameters have shown promise in providing valuable insights for classification and diagnosis. These findings open avenues for further research and clinical applications in managing MRIn-MTLE among athletes and fitness enthusiasts.

As our knowledge continues to evolve, a multidisciplinary approach involving neurologists, sports medicine specialists, and imaging experts becomes increasingly important in addressing the unique challenges posed by MRIn-MTLE within this population. By better understanding the structural brain changes associated with MRIn-MTLE, we can enhance diagnostic accuracy and develop more targeted interventions, ultimately improving the quality of life for athletes and fitness enthusiasts affected by this condition

Declarations

Ethics approval and consent to participate

This research was authorized by the Medical Research Ethics Board of First Affiliated Hospital of Xinjiang Medical University, all methods were performed in accordance with the relevant guidelines and regulations, and all subjects provided written informed consent forms.

Consent for publication

All subjects including children's parents provided written informed consent forms, terms regarding publication consent were included in the consent form.

Availability of data and materials

The datasets used and/or analysed during the current study are available from the corresponding author on reasonable request.

Competing interests

The authors declare that the research was conducted in the absence of any commercial or financial relationships that could be construed as a potential conflict of interest.

Funding

This work was supported by Regional Collaborative Innovation special fund of Xinjiang Uygur Autonomous Region (Grant: #2020E0275), and Xinjiang Uygur Autonomous Region Natural Science Foundation Science Fund project (Grant: #2022D01C774)

Authors' contributions

HK wrote the first version of this manuscript. FY and SD carried out the data processing and statistical analysis. HZ was responsible for the data collection. WJ and YW contributed to the conception and design of this manuscript. All authors contributed to the manuscript revision.

Acknowledgements

Not applicable

Project Support：

1.Regional Collaborative Innovation special fund of Xinjiang Uygur Autonomous Region (Grant: #2020E0275),

2.Xinjiang Uygur Autonomous Region Natural Science Foundation Science Fund project (Grant: #2022D01C774)

REFERENCES

Alvim, M. K., Coan, A. C., Campos, B. M., Yasuda, C. L., Oliveira, M. C., Morita, M. E., & Cendes, F. (2016). Progression of gray matter atrophy in seizure-free patients with temporal lobe epilepsy. *Epilepsia, 57*(4), 621-629.

Balter, S., Lin, G., Leyden, K., Paul, B., & McDonald, C. (2019). Neuroimaging correlates of language network impairment and reorganization in temporal lobe epilepsy. *Brain and Language, 193*, 31-44.

Berg, A. T., Berkovic, S. F., Brodie, M. J., Buchhalter, J., Cross, J. H., van Emde Boas, W., . . . Mathern, G. W. (2010). Revised terminology and concepts for organization of seizures and epilepsies: report of the ILAE Commission on Classification and Terminology, 2005–2009. In: Wiley Online Library.

Cendes, F. (2005). Mesial temporal lobe epilepsy syndrome: an updated overview. *Journal of Epilepsy and Clinical Neurophysiology, 11*, 141-144.

Englot, D. J., Konrad, P. E., & Morgan, V. L. (2016). Regional and global connectivity disturbances in focal epilepsy, related neurocognitive sequelae, and potential mechanistic underpinnings. *Epilepsia, 57*(10), 1546-1557.

Fischl, B. (2012). FreeSurfer. *Neuroimage, 62*(2), 774-781.

Fischl, B., Salat, D. H., Busa, E., Albert, M., Dieterich, M., Haselgrove, C., . . . Klaveness, S. (2002). Whole brain segmentation: automated labeling of neuroanatomical structures in the human brain. *Neuron, 33*(3), 341-355.

Herman, J., McKlveen, J., Ghosal, S., Kopp, B., Wulsin, A., Makinson, R., . . . Myers, B. (2016). Regulation of the hypothalamic-pituitary-adrenocortical stress response. Compr Physiol 6: 603–621. In.

Jones, A. L., & Cascino, G. D. (2016). Evidence on use of neuroimaging for surgical treatment of temporal lobe epilepsy: a systematic review. *JAMA neurology, 73*(4), 464-470.

Morris, R. (2006). Elements of a neurobiological theory of hippocampal function: the role of synaptic plasticity, synaptic tagging and schemas. *European Journal of Neuroscience, 23*(11), 2829-2846.

Natsume, J., Bernasconi, N., Andermann, F., & Bernasconi, A. (2003). MRI volumetry of the thalamus in temporal, extratemporal, and idiopathic generalized epilepsy. *Neurology, 60*(8), 1296-1300.

Pardoe, H. R., Berg, A. T., & Jackson, G. D. (2013). Sodium valproate use is associated with reduced parietal lobe thickness and brain volume. *Neurology, 80*(20), 1895-1900.

Pitts, P. J. (2022). Rejuvenating American Healthcare: An Honest Debate. *Journal of Commercial Biotechnology, 27*(1).

Sáiz-Manzanares, M.-C., Casanova, J., Lencastre, J.-A., & Almeida, L. (2022). Student satisfaction with online teaching in times of COVID-19. *Comunicar, 30*(70), 35-45.

Sämann, P. G., Iglesias, J. E., Gutman, B., Grotegerd, D., Leenings, R., Flint, C., . . . van Erp, T. G. (2022). FreeSurfer‐based segmentation of hippocampal subfields: A review of methods and applications, with a novel quality control procedure for ENIGMA studies and other collaborative efforts. *Human brain mapping, 43*(1), 207-233.

Song, Y., Zhang, J., Zhang, Y.-d., Hou, Y., Yan, X., Wang, Y., . . . Yang, G. (2020). FeAture Explorer (FAE): a tool for developing and comparing radiomics models. *PLoS One, 15*(8), e0237587.

Stefanits, H., Springer, E., Pataraia, E., Baumgartner, C., Hainfellner, J. A., Prayer, D., . . . Trattnig, S. (2017). Seven-tesla MRI of hippocampal sclerosis: an in vivo feasibility study with histological correlations. *Investigative radiology, 52*(11), 666-671.

Steve, T. A., Gargula, J., Misaghi, E., Nowacki, T. A., Schmitt, L. M., Wheatley, B. M., & Gross, D. W. (2020). Hippocampal subfield measurement and ILAE hippocampal sclerosis subtype classification with in vivo 4.7 tesla MRI. *Epilepsy research, 161*, 106279.

Thom, M. (2014). Hippocampal sclerosis in epilepsy: a neuropathology review.

Neuropathology and applied neurobiology, 40(5), 520-543.

Tondelli, M., Vaudano, A. E., Sisodiya, S. M., & Meletti, S. (2020). Valproate use is associated with posterior cortical thinning and ventricular enlargement in epilepsy patients. *Frontiers in neurology, 11*, 622.

Varho, T., Komu, M., Sonninen, P., Lähdetie, J., & Holopainen, I. E. (2005). Quantitative 1HMRS and MRI volumetry indicate neuronal damage in the hippocampus of children with focal epilepsy and infrequent seizures. *Epilepsia, 46*(5), 696-703.

Wiebe, S., Blume, W. T., Girvin, J. P., & Eliasziw, M. (2001). A randomized, controlled trial of surgery for temporal-lobe epilepsy. *New England Journal of Medicine, 345*(5), 311-318.

Wu, W.-C., Huang, C.-C., Chung, H.-W., Liou, M., Hsueh, C.-J., Lee, C.-S., . . . Chen, C.-Y. (2005). Hippocampal alterations in children with temporal lobe epilepsy with or without a history of febrile convulsions: evaluations with MR volumetry and proton MR spectroscopy. *American journal of neuroradiology, 26*(5), 1270-1275.